Electronic Supplementary Material (ESI) for Journal of Materials Chemistry A.

Supporting Information

Recruiting Physisorbed Water in surface Polymerization for Bio-Inspired Materials of Tunable Hydrophobicity

Stephanie Oyola-Reynoso[a], Ian D. Tevis[a], Jiahao Chen[a,b,c], Boyce S. Chang[a,c], Simge Çınar[a], Jean-Francis Bloch[e], Martin M. Thuo[a,b,c,d*]

AFFILIATIONS

a. Department of Materials Science and Engineering, Iowa State University, Ames, IA 50011
b. Micro-electronic research center, Iowa State University, 133 Applied Sciences Complex I, 1925 Scholl Road, Ames, IA 50011 USA
c. Ames Lab, 134 Wilhelm Hall, Iowa State University, Ames, IA 50011
d. Biopolymer and Biocomposites Research Team, Center for Bioplastics and Biocomposites, Iowa State University, 1041 Food Sciences Building, Ames, IA 50011 USA
e. University of Grenoble, 461 Rue de la Papeterie. 38402 Saint-Martin-d'Heres, France

[*]Corresponding author E-mail: mthuo@iastate.edu

Step-Growth Polymerization for Gel Formation

While biphobic surfaces have a wide array of applications,[1-8] methods to fabricate these important materials has often employed complicated or expensive methods or technology.[5, 7, 9-12] Self-assembled monolayers, on the other hand, have been used successfully in modifying surface energy of myriad materials and utilize well know chemical reactions and molecular self-assembly to give well-defined surfaces and interfaces.[13-18] Nature, like in the Namib beetle,[19, 20] uses a similar approach, i.e. self-assembly and simple interface chemistry, to make amphiphobic surfaces. Nature, however, is geared towards water harvesting (e.g. insects in xeric environments)[19, 20] or self-cleaning (e.g. plants),[21] while many man-made systems, e.g. increased use of fossil fuels, and related products, has led to an increase in environmental aerosols hence the need for surface that can sequester non-polar materials. We term these type of surfaces as inverse-Namib beetle (*i*-NB), that is; surfaces with hydrophobic bumps and hydrophilic trenches. We are interested in such surfaces and sought to develop a general technique of fabricating biphobic and/or biphillic surfaces.

Gel-formation in Silanes Bearing Multiple Reactive Sites: Since water has two reactive sites while an alkyl trichlorosilane has three (for equimolar quantities, the total number of reactive moieties per mole, f, = 5), the critical coefficient of branching, α_c, for gel formation is 0.25. To satisfy the gel formation condition ($\alpha(f\text{-}1) \geq 1$), and assuming that at least one of the monomers is fully consumed, the ratios of the two monomers should be at least 1:4 (Equation 1), for crosslinking with gel formation to occur.

$$\alpha = \frac{r\rho P_A^2}{1-r(1-\rho)P_A^2} \cdots\cdots\cdots\cdots\cdots\cdots\cdots\cdots\cdots\cdots\cdots \quad (1)$$

Where P_A is the probability of functional group A being in the gel, ρ is the probability of a moiety being in the branches of the gel, and, *r* is the ratio of the total number of reacting functionalities.

Step-growth polymerization, however, is plagued by the paradox inherent in Carothers equation, that is, high degree of polymerization is only possible at significantly high conversions. In our case, however, this paradox suggests good control over the degree of polymerization, hence, an ability to control the size of particles forming on the surface. We, therefore, hypothesized that under the proposed surface functionalization process, the size of surface adsorbed particles can be controlled by controlling the degree of polymerization.

$$x_n = \frac{1+r}{1+r-2rp} \quad \cdots\cdots\cdots\cdots\cdots\cdots\cdots\cdots\cdots\cdots\cdots\cdots\cdots\cdots\cdots\cdots\cdots \quad (2)$$

Where x_n is the degree of polymerization, r is the ratio of the two reacting moieties and p is the extent of reaction of one of the reactive moieties.

We therefore hypothesized that the covalent attachment of an alkyl trichlorosilane on paper (cellulose) should be preceded by oligomerization and/or cross-linking by surface adsorbed water, followed by concomitant self-assembly of the oligomeric/polymerized chains, to give particles of different sizes and shapes.

Grammage values: Grammage is the value of the fiber per unit area found on paper. Calculated as follow,

$$Grammage = \frac{g}{m^2}$$

$$Grammage\ Filter\ paper = \frac{0.5011g}{0.09\ m\ x\ 0.06\ m} = 92.79\ {}^{g}/_{m^2}$$

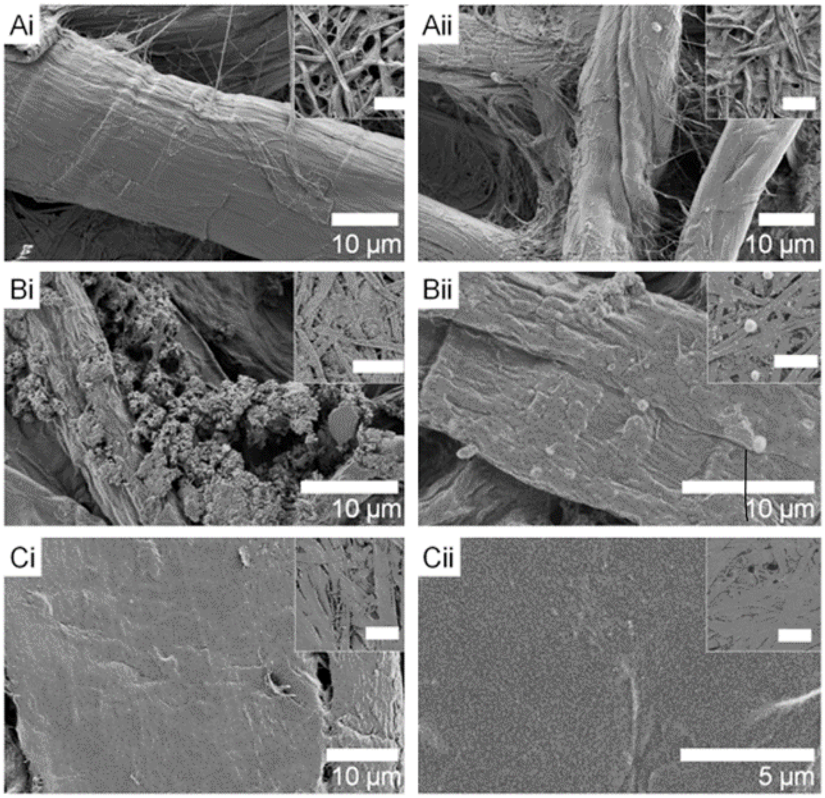

Figure *S1*: SEM micrograph of chemical modification of representative types of paper before treatment (i) and the analogous paper after treatment with trichlorooctylsilane (ii. All insets are a low magnification SEM micrograph of the paper with a scale bar of 100 µm. Ai) Highly porous predominantly cellulose paper represented here by chromatography paper #1 (grammage = 92 g/m^2). Aii) On chemical modification no change in surface texture is observed. Bi) A porous paper containing filler materials represented by cardstock paper, which contains PCC filler. Bii) On silanization large and small particles are observed. Ci) Dense (grammage = 16 g/m^2) paper represented by the NYX blotting paper. Cii) Upon silanization small particles can be observed.

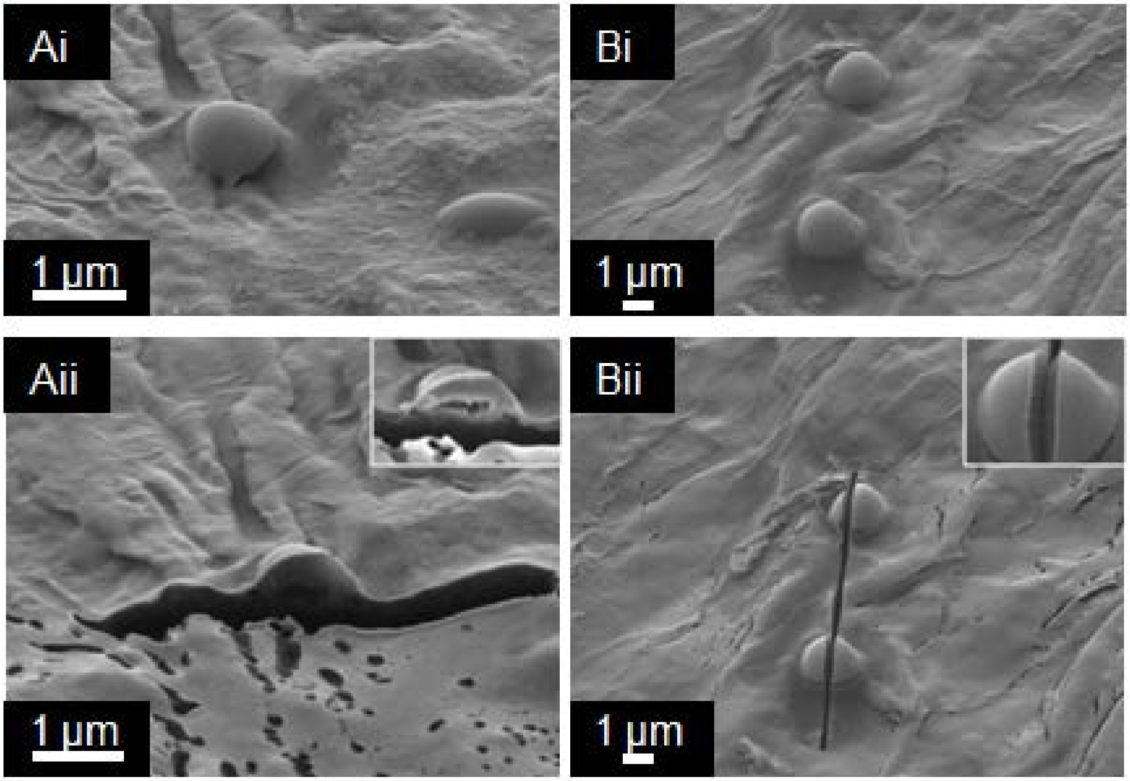

Figure S2: Non-colorized version of Figure 4. SEM micrographs of large fluoroalkyl polymers before and after milling using a focused ion beam. Ai) Two microparticles. Aii) The largest particle was milled in half to reveal a solid core with a small gap forming underneath it seen in the inset. Inset is 2.1 µm across. Bi) Two additional microparticles. Bii) Both particles are partially milled down the center to show that the particles are solid and not bubbles see higher magnification inset. Inset is 2.4 µm across.

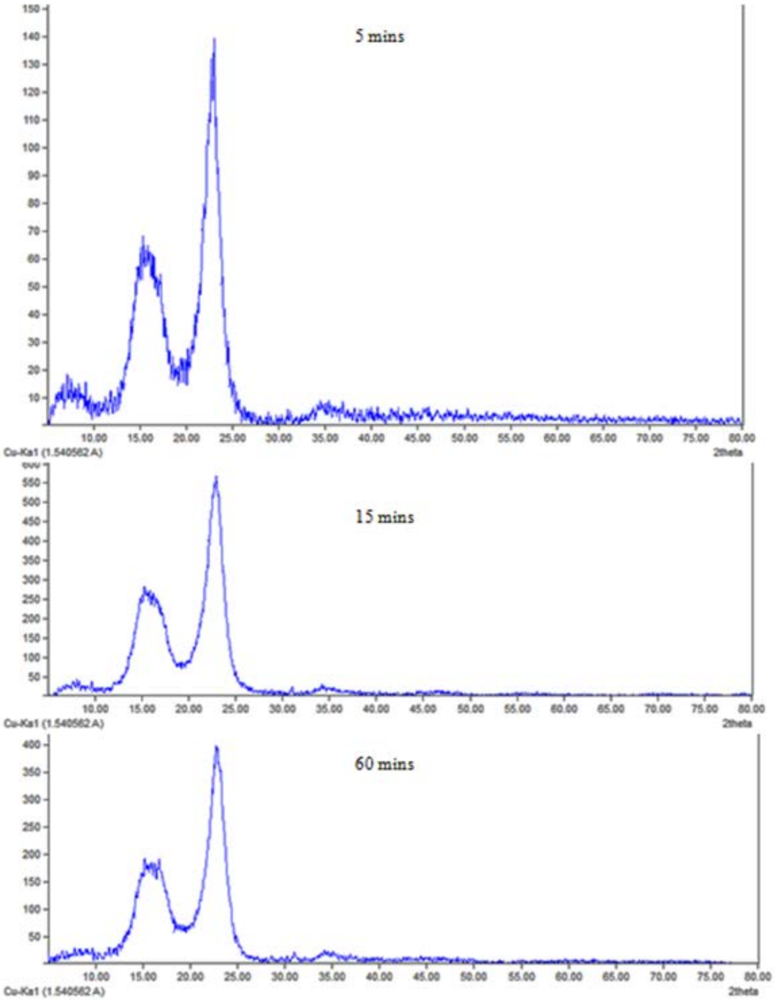

Figure S3: X-ray diffraction shows no significant change in the crystallinity of the polymer (cellulose), from which the paper is made, after treatment. The similarity between XRD diffraction patterns between treated and untreated materials indicates that the particles formed from silanization have not significantly altered the structure of the solid paper and are a minor component in the material.

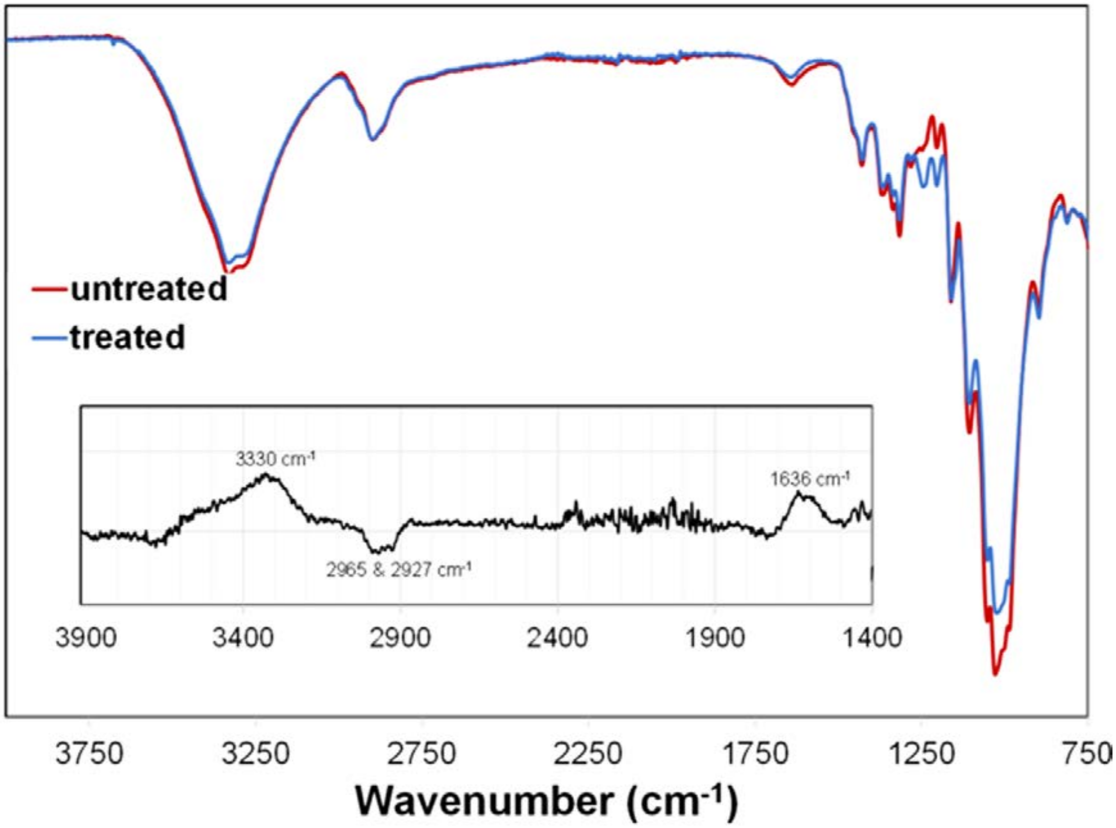

Figure S4 : FTIR analysis of treated and untreated paper with the difference in the two spectra shown in the insert. Three major differences are highlighted and labeled, the OH stretch and scissoring (negative peaks) and the C-H str (positive peak) are highlighted. The slight difference in the changes in –OH peaks indicates that only a small amount of the hydroxyls has been silanized hence no significant effect on the overall mechanical properties or appearance of the treated paper.

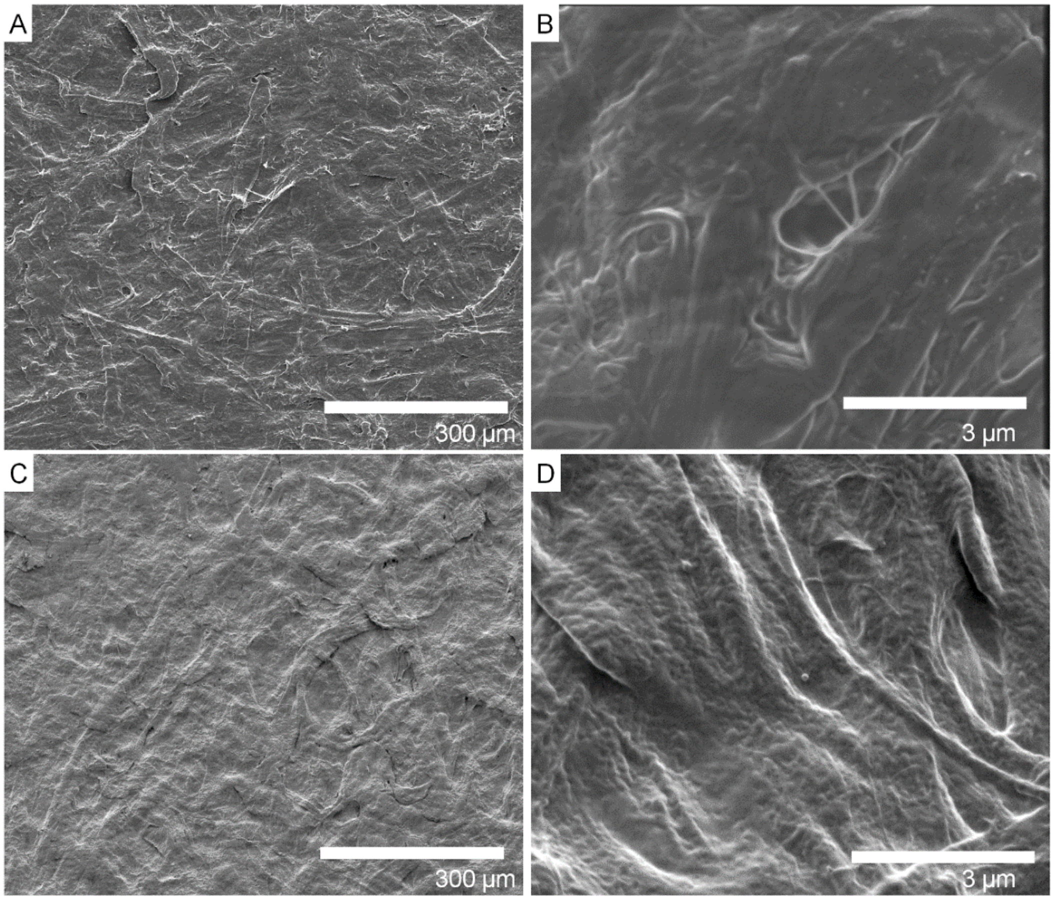

Figure S5: High-density paper (grammage = 79 g/m^2) before and after treatment with fluorosilane vapor for 1 hour at 95 °C. A) Low and B) high magnification SEM micrographs of paper before treatment. C) Low and D) high magnification images of the paper after treatment showing a slight change in surface texture but no significant particle formation.

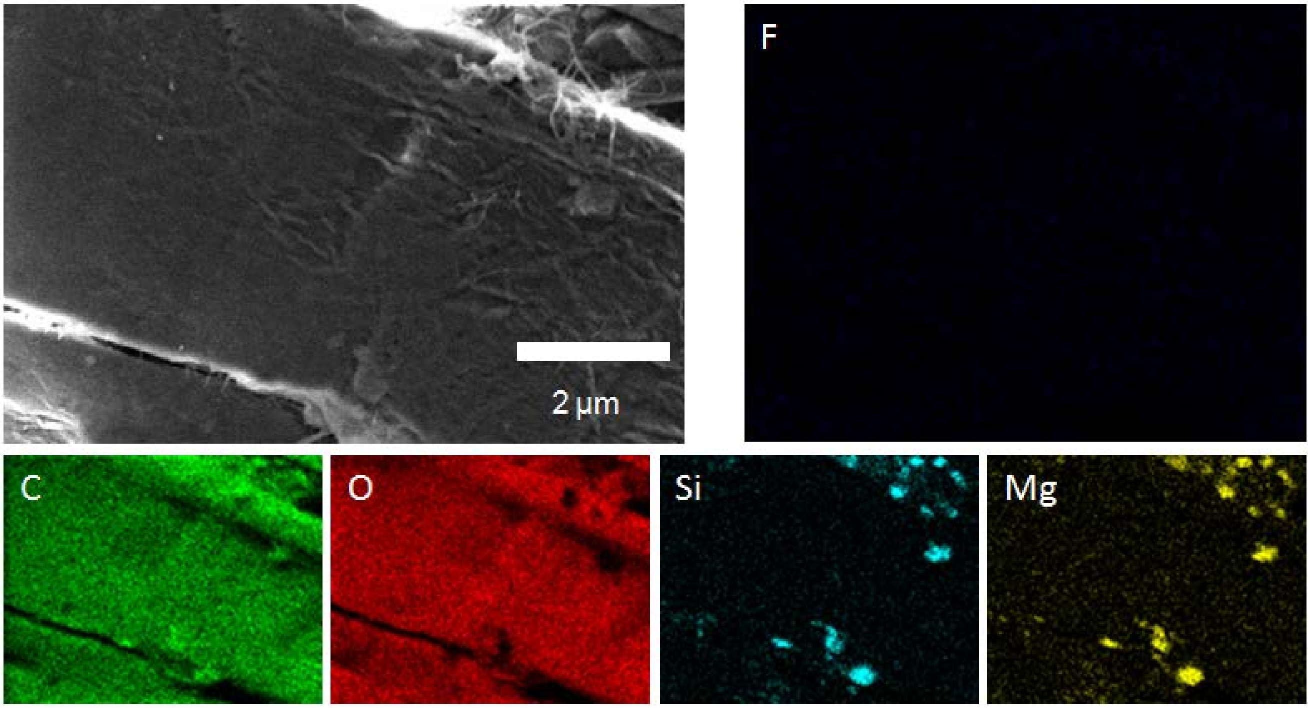

Figure S6: SEM and EDS elemental mapping of the untreated NYX blotting paper. There is no observable amount of fluorine in the sample, however, small amounts of adventitious silicon and magnesium are present.

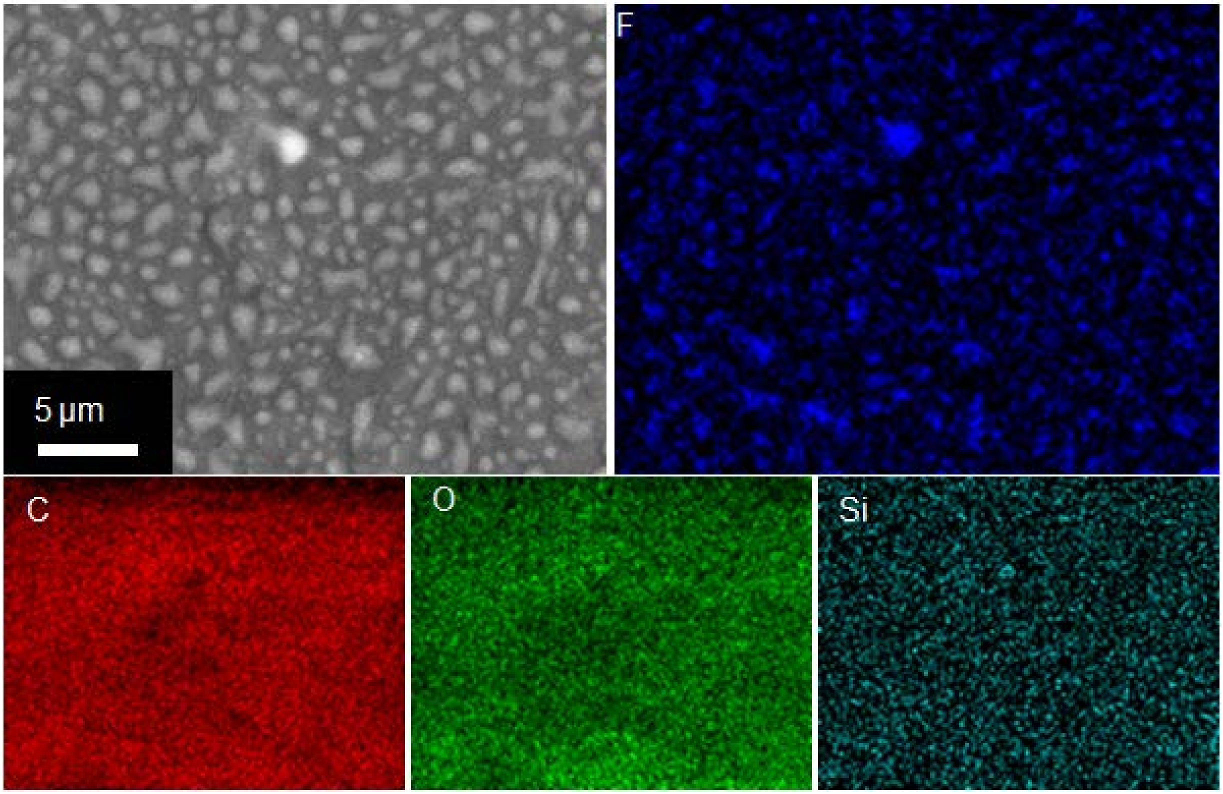

Figure S7: SEM and EDS elemental mapping of the treated NYX blotting paper. The SEM image of the treated paper alongside the distribution map of fluorine showing a good correlation in the spatial distribution of the particle and fluorine element. As expected, C and O are distributed all over the paper, while Si, with the observed adventitious amount, is also not correlating with the particles but is of a much reduced amount compared to C and O.

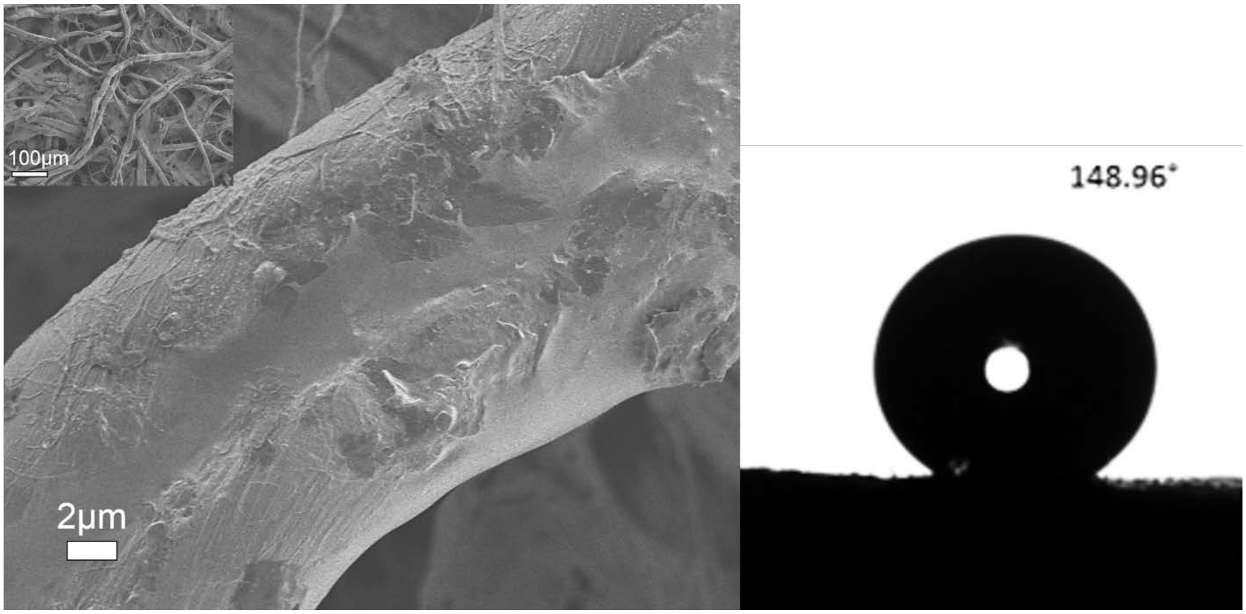

Figure S8. SEM images and water contact angles derived from ultra-hydrophobic filter paper (grammage = 92 g/m^2) after treatment with the perfluoro octyltrichlorosilane for 24 hours at 95 °C.

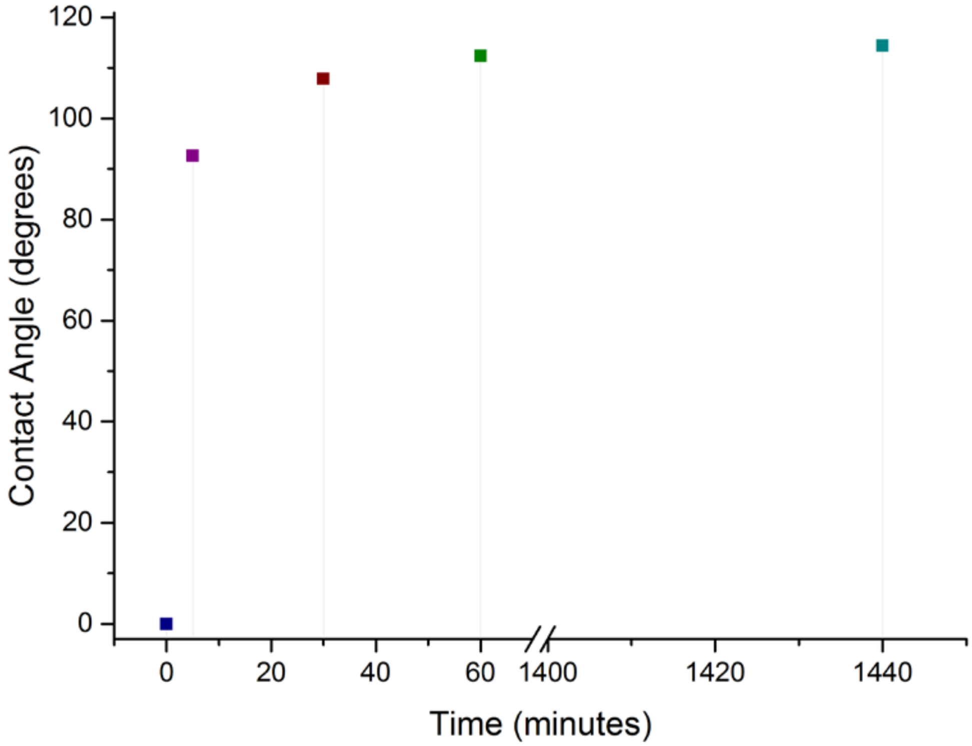

Figure S9. Contact Angle of both unmodified and modified dense blotting paper for perfluorinated silane.

REFERENCES:

1. E. K. Her, T.-J. Ko, K.-R. Lee, K. H. Oh and M.-W. Moon, *Nanoscale*, 2012, **4**, 2900-2905.
2. J. L. Plawsky, J. K. Kim and E. F. Schubert, *Materials Today*, 2009, **12**, 36-45.
3. Y. Wang, L. Zhang, J. Wu, M. N. Hedhili and P. Wang, *J. Mater. Chem. A*, 2015, **3**, 18963-18969.
4. L. Zhai, M. C. Berg, F. C. Cebeci, Y. Kim, J. M. Milwid, M. F. Rubner and R. E. Cohen, *Nano Letters*, 2006, **6**, 1213-1217.
5. Y. Zheng, C. Su, J. Lu and K. P. Loh, *Angew. Chem., Int. Ed.*, 2013, **52**, 8708-8712.
6. L. Eadie and T. K. Ghosh, *Journal of the Royal Society Interface*, 2011, **8**, 761-775.
7. Y. Liu, X. Yin, J. Zhang, Y. Wang, Z. Han and L. Ren, *Appl. Surf. Sci.*, 2013, **280**, 845-849.
8. M. Sarkar, J. Fan, Y.-c. Szeto and X. Tao, *Textile Research Journal*, 2009, **79**, 657-668.
9. A. G. Cunha and A. Gandini, *Cellulose*, 2010, **17**, 875-889.
10. C. Ganser, F. Weber, C. Czibula, I. Bernt, R. Schennach and C. Teichert, *Bioinspired Biomimetic and Nanobiomaterials*, 2014, **3**, 131-138.
11. G. Sun and Y. Fang, *Appl. Mech. Mater.*, 2015, **727-728**, 3-6, 5 pp.
12. S. C. Thickett, C. Neto and A. T. Harris, *Adv. Mater.*, 2011, **23**, 3718-+.
13. A. Hozumi, K. Ushiyama, H. Sugimura and O. Takai, *Langmuir*, 1999, **15**, 7600-7604.
14. M. Karakoy, E. Gultepe, S. Pandey, M. A. Khashab and D. H. Gracias, *Appl. Surf. Sci.*, 2014, **311**, 684-689.
15. K. L. Mittal, *Silanes and other coupling agents*, CRC Press, 2007.
16. V. V. Naik, R. Stadler and N. D. Spencer, *Langmuir*, 2014, **30**, 14824-14831.
17. C. Zhang, N. E. Shephard, S. M. Rhodes and Z. Chen, *Langmuir*, 2012, **28**, 6052-6059.
18. H. Zhou, H. Wang, H. Niu, A. Gestos, X. Wang and T. Lin, *Adv. Mater.*, 2012, **24**, 2409-2412.
19. J. Guadarrama-Cetina, A. Mongruel, M. G. Medici, E. Baquero, A. R. Parker, I. Milimouk-Melnytchuk, W. Gonzalez-Vinas and D. Beysens, *Eur. Phys. J. E Soft Matter Biol. Phys.*, 2014, **37**, 1-6.
20. M. K. Seely and W. J. Hamilton, *Science*, 1976, **193**, 484-486.
21. Y. Choi, T. Brugarolas, S.-M. Kang, B. J. Park, B.-S. Kim, C.-S. Lee and D. Lee, *ACS Appl. Mater. Interfaces*, 2014, **6**, 7009-7013.